ELSEVIER

Three-dimensional seismic modelling of crustal structure in the TESZ region based on POLONAISE'97 data

Piotr Środa [a,*], Wojciech Czuba [a], Marek Grad [b],
Aleksander Guterch [a], Edward Gaczyński [a]
POLONAISE Working Group [1]

[a]*Institute of Geophysics, Polish Academy of Sciences, Ks. Janusza 64, 01-452 Warsaw, Poland*
[b]*Institute of Geophysics, University of Warsaw, Pasteura 7, 02-093 Warsaw, Poland*

Abstract

This paper reports the results of 3-D tomographic modelling of crustal structure in the Trans European Suture Zone region (TESZ) of Poland, eastern Germany and Lithuania. The data are the product of a large-scale seismic experiment POLONAISE'97, which was carried out in 1997. This experiment was designed to provide some 3-D coverage. The TESZ forms the boundary between the Precambrian crustal terranes of the East European Craton (EEC) and the younger Phanerozoic terranes to the southwest. The 3-D results generally confirm the earth models derived by earlier 2-D analyses, but also add some important details as well as a 3-D perspective on the structure. The velocity model obtained shows substantial horizontal variations of crustal structure across the study area. Seismic modelling shows low (< 6.1 km/s) velocities suggesting the presence of sedimentary rocks down to a depth of about 20 km in the Polish basin. The shape of the basin in the vicinity of the profile P4 shows significant asymmetry. Three-dimensional modelling also allowed tracing of horizontal irregularities of the basin shape as well as variations of the Moho depth not only along profiles, but also between them. The slice between P2 and P4 profiles shows about 10-km variations of the Moho over a 100-km interval. The crustal thickness varies from about 30 km in SW, beneath the Palaeozoic platform, to about 42 km beneath East European Craton in NE. High seismic velocities of about 6.6 km/s were found in the depth range 2–10 km, which coincides with Kętrzyn anorthosite massif. The results of this 3-D seismic modelling of the POLONAISE'97 data will ultimately be supplemented by inversion of seismic data from previous experiments.
© 2002 Elsevier Science B.V. All rights reserved.

Keywords: Seismic; Crust; Moho

* Corresponding author. Tel.: +48-22-691-5950; fax: +48-22-691-5915.
E-mail address: psroda@igf.edu.pl (P. Środa).

1. Introduction

The study area spans Poland, eastern Germany and Lithuania (Fig. 1), as well as the boundary between the Precambrian crustal terranes of the East European Craton (EEC) and the younger Phanerozoic terranes to the southwest. This boundary has come to be known as the Trans European Suture Zone (TESZ) (Berthelsen, 1992a,b, 1998; Pharaoh et al., 1997). A number of major tectonic features are found within the TESZ region. Of particular interest in this study is the Permian basin that covers a large part of Poland and northern Germany. This basin was filled with more than 10 km of Permian and Mesozoic sedimen-

tary rocks during a phase of extension and subsidence after the Variscan orogeny. The Polish basin is the easternmost subbasin of the Permian basin and is bounded on the southwest by the Bohemian massif (Dadlez, 1989; Ziegler, 1990; Pharaoh et al., 1997). The axial area of this basin has a long history of systematic subsidence (thermal, shelf subsidence) that began in the Early Palaeozoic (and probably from the Late Precambrian). In recent tectonic investigations, the structural framework and tectonic evolution of the Polish Basin has been interpreted in slightly different ways by Kutek (1997) and Karnkowski (1999). Kutek (1997) suggests that the basin consists of an asymmetrical fault-bounded rift structure and a superim-
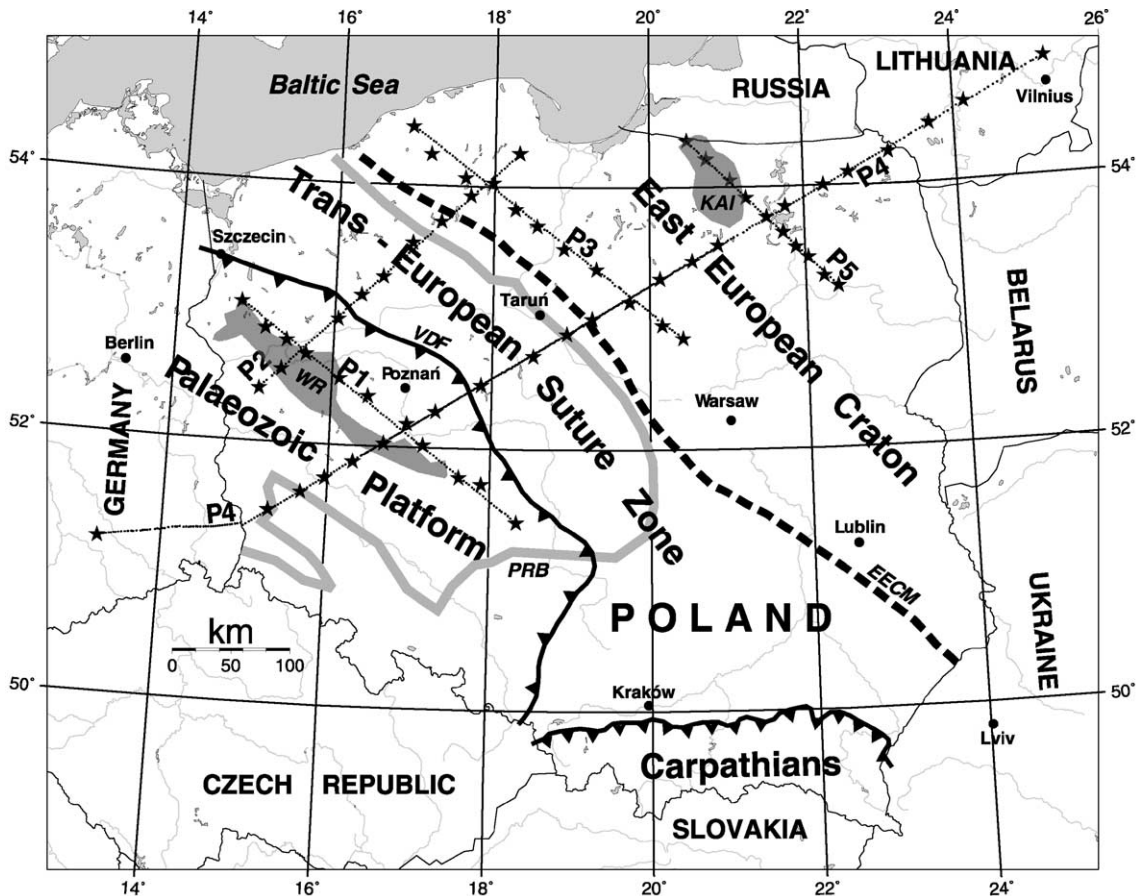
Fig. 1. Location of the POLONAISE'97 profiles P1, P2, P3 P4 and P5. Shot points are marked by stars and recording stations by points. EECM, East European Craton Margin. VDF, Variscan Deformation Front. Gray line: PRB—present extent of the Polish Rotliegend Basin (Karnkowski, 1999). Gray areas: WR—Wolsztyn Ridge, KAI—Kętrzyn Anorthosite Intrusion.

posed Upper Cretaceous sag basin. Karnkowski (1999) interprets this basin as an asymmetric rift structure formed by simple-shear (Wernicke, 1981, 1985), with associated volcanism at 290–270 Ma (Early/Late Permian).

2. Previous seismic investigations

The TESZ–Polish Basin region has been the target of a number of deep seismic investigations prior to the POLONAISE'97 effort that will be discussed below.
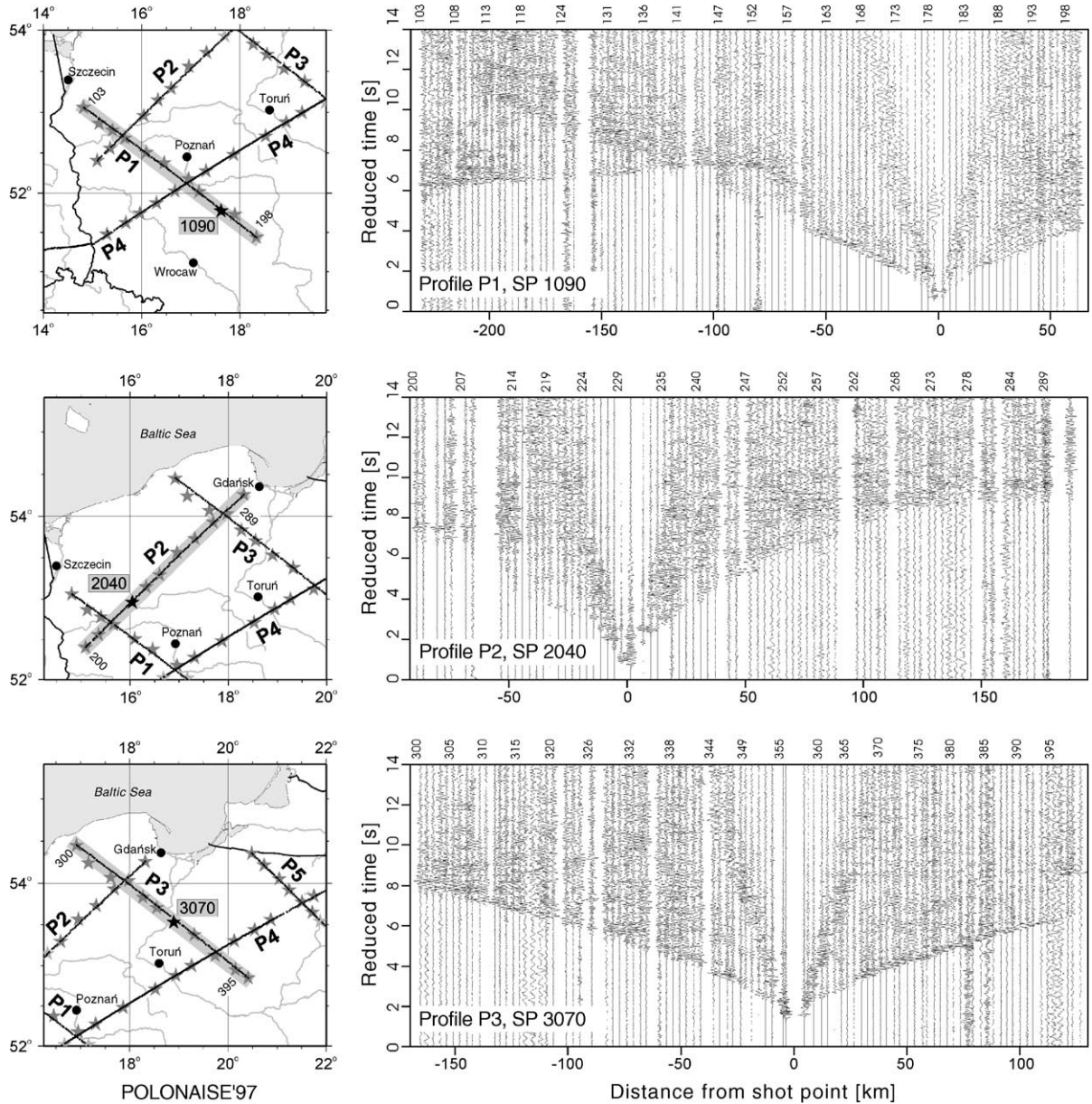
Fig. 2. Examples of seismic record sections from in-line shots: along profile P1 for SP 1090 (upper), profile P2 for SP 2040 (middle) and profile P3 for SP 3070 (bottom), and their corresponding locations (gray thick lines in maps in the left) with shots (black stars) and both end station numbers. Reduction velocity is 8 km/s, traces are normalized to maximum amplitude. Band-pass filter 2–15 Hz was applied.

These data provide useful information on crustal structure but do not have the resolution provided by the large number of receivers and sources used during POLONAISE'97. The deep crustal structure of the Polish basin is characterised by crustal thickening beneath the central part of the basin (Guterch et al., 1986), as well as crustal thinning beneath the northwest part of the basin (Guterch et al., 1992, 1994). In
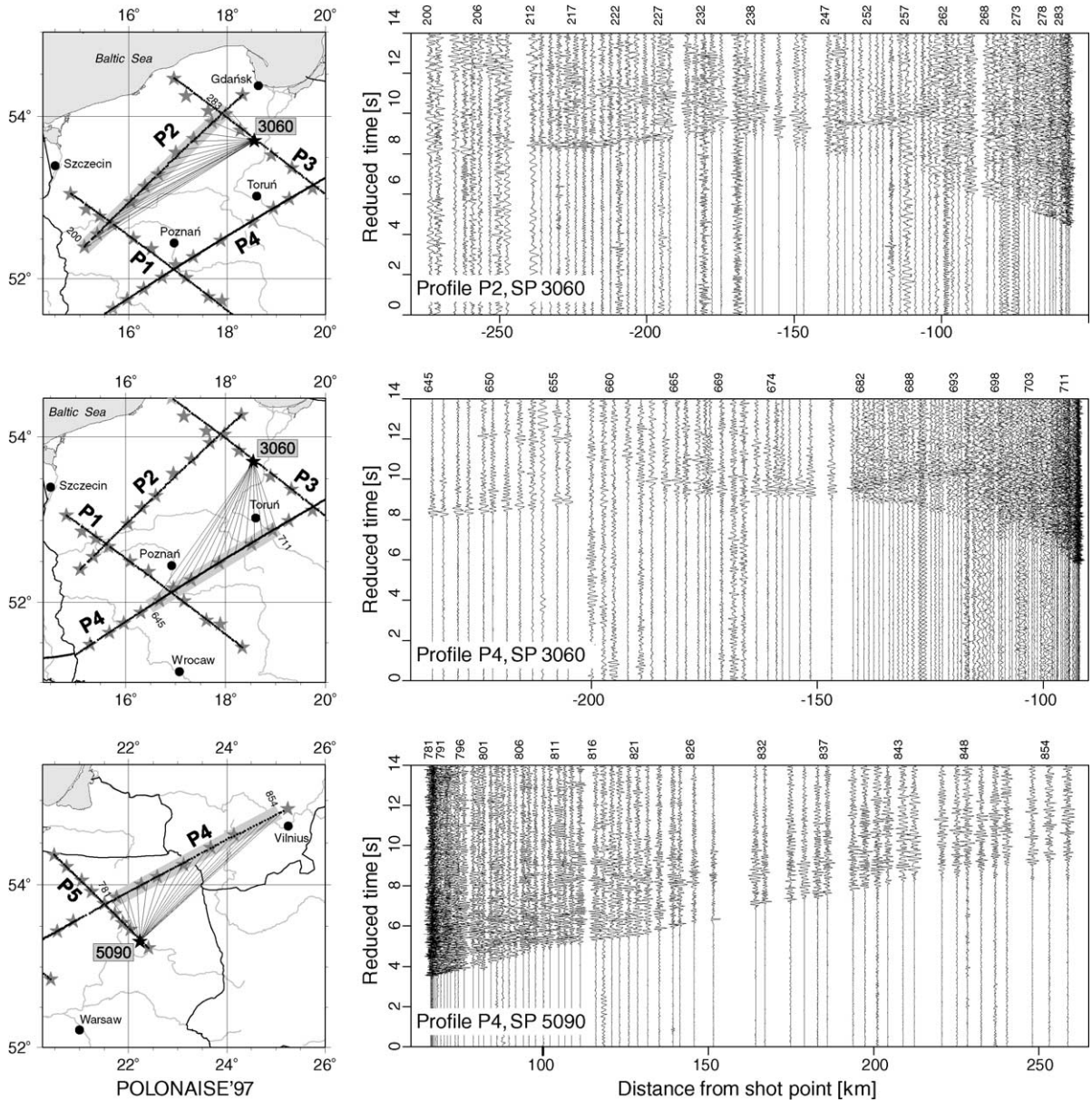
Fig. 3. Examples of seismic record sections recorded from fan shots: along profile P2 for SP 3060 from profile P3 (upper), along profile P4 for SP 3060 from profile P3 (middle) and along profile P4 for SP 5090 from profile P5 (bottom). Locations of profiles (gray thick lines) with both end station numbers and shots (black stars) are shown on maps (in the left). Lines symbolize raypaths between shot and stations. Reduction velocity is 8 km/s, traces are normalized to maximum amplitude. Band-pass filter 2–15 Hz was applied.

northwesternmost Poland, the results from the LT-7 seismic profile show that the crustal thickness near the TESZ is intermediate between that of the East Euro-pean Craton to the northeast (~ 42 km) and that in the area to the southwest (~ 30 km) near the Polish/German border (Guterch et al., 1994; Guterch and
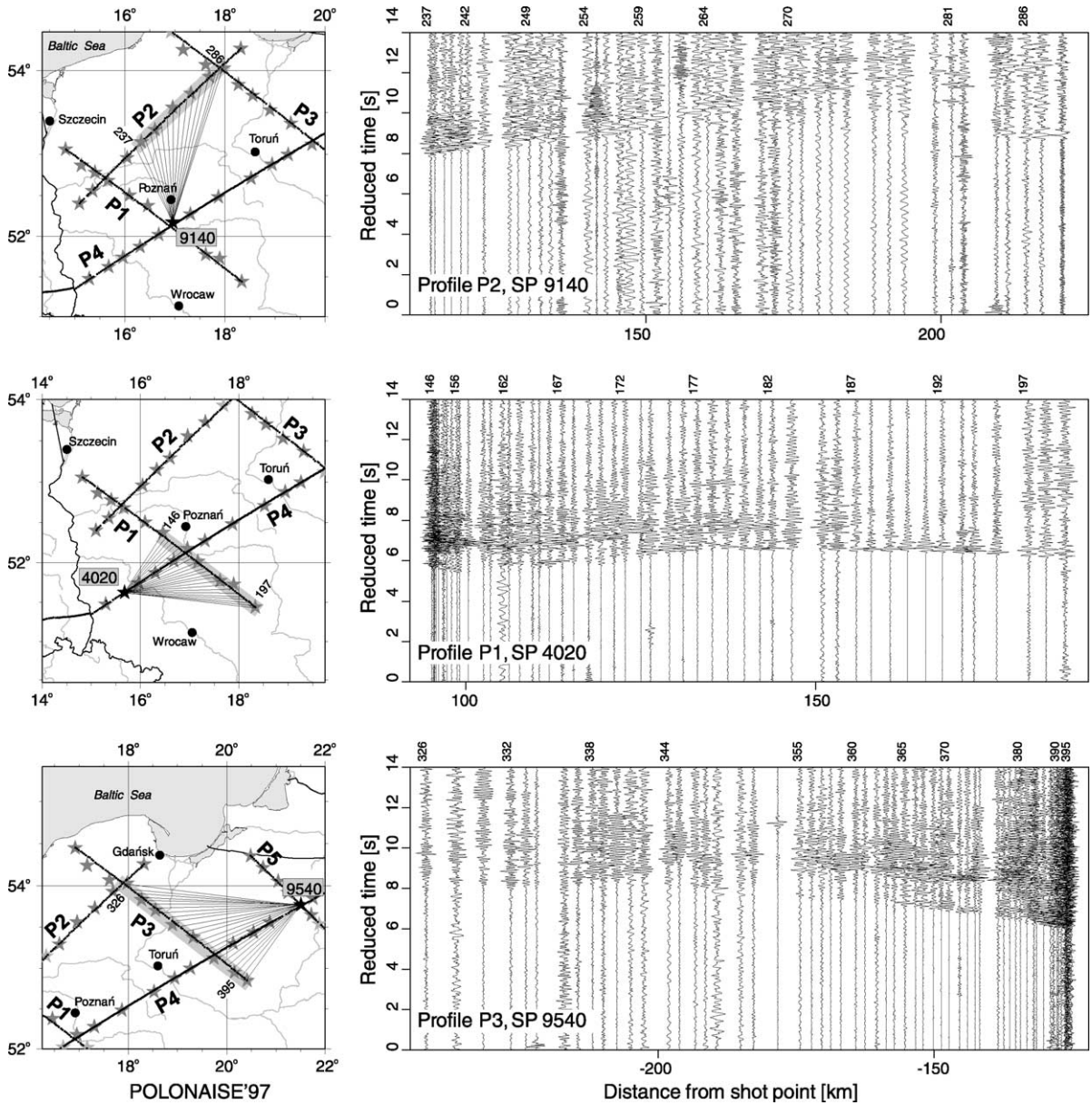
Fig. 4. Examples of seismic record sections from fan shots: along northern part of profile P2 for SP 9140 from profile P1/P4 (upper), along eastern part of profile P1 for SP 4020 from profile P4 (middle) and along eastern part of profile P3 for SP 9540 from profile P4/P5 (bottom). Locations of profiles (gray thick lines) with both end station numbers and shots (black stars) are shown on maps (in the left). Lines symbolize raypaths between shot and stations. Reduction velocity is 8 km/s, traces are normalized to maximum amplitude. Band-pass filter 2–15 Hz was applied.

Grad, 1996). The LT-7 profile is crossed by the northwest-trending TTZ profile that approximately follows the deepest portion of the Polish Basin (Grad

et al., 1999). The velocity model derived from the TTZ experiment showed that the crustal thickness varied from 37 to 41 km and that low velocities
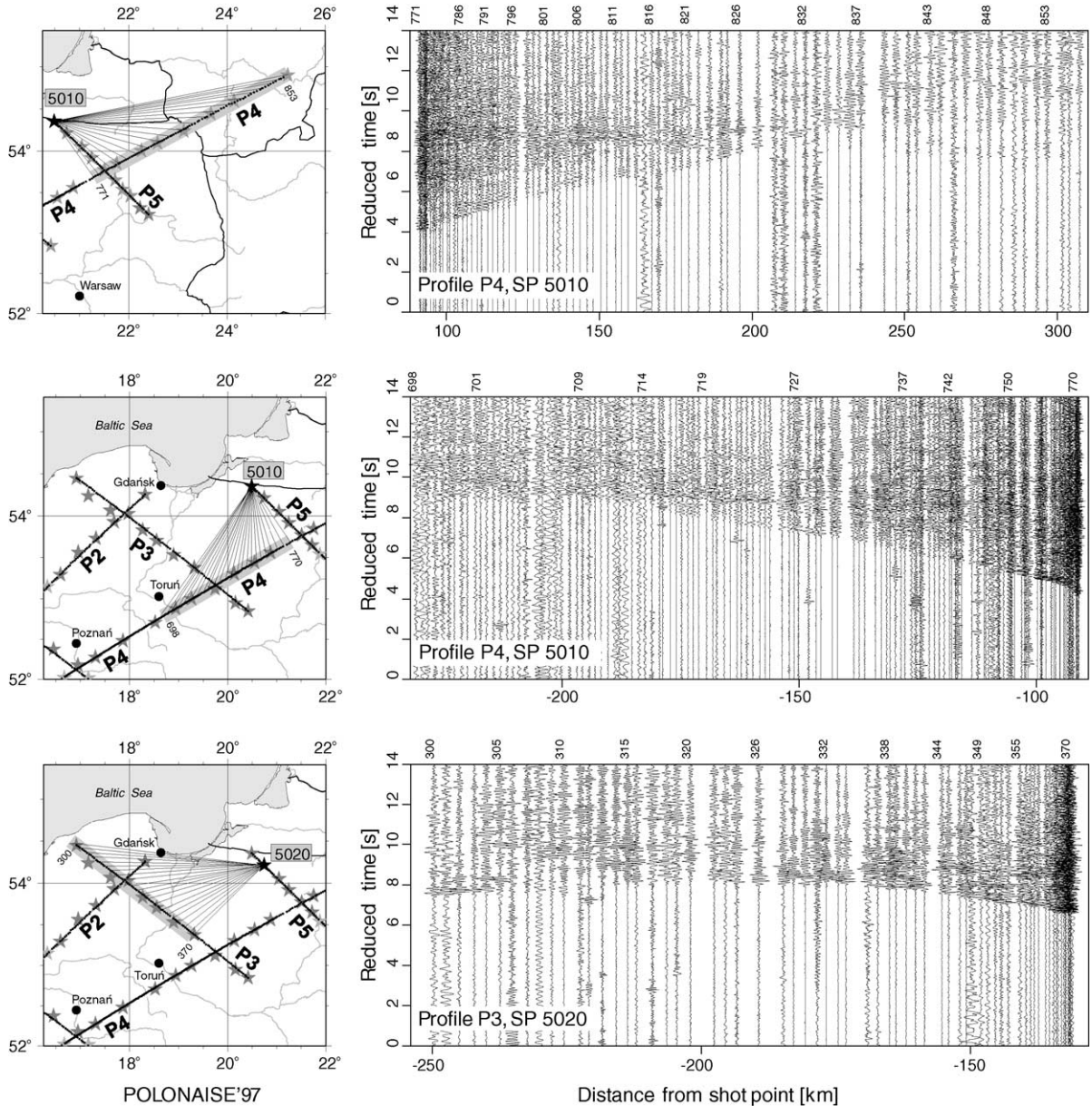
Fig. 5. Examples of seismic record sections from fan shots: along northern part of profile P4 for SP 5010 from profile P5 (upper), along central part of profile P4 for SP 5010 from profile P5 (middle) and along western part of profile P2 for SP 5020 from profile P5 (bottom). Locations of profiles (gray thick lines) with both end station numbers and shots (black stars) are shown on maps (in the left). Lines symbolize raypaths between shot and stations. Reduction velocity is 8 km/s, traces are normalized to maximum amplitude. Band-pass filter 2–15 Hz was applied.

(<6.1 km/s) extended to depths of 15–20 km. In central and southeastern Poland, early deep seismic sounding (DSS) studies show that the TESZ is associated with a crustal root in which the thickness locally exceeds 50 km (Guterch et al., 1986).

The large-scale seismic experiment POLONAISE'97 conducted in May 1997 targeted the deep structure of the TESZ in northwestern Poland (Guterch et al., 1997, 1998) and the first results were presented by Guterch et al. (1999), Jensen et al. (1999), Šroda and POLONAISE Working Group (1999), Wilde-Piórko et al. (1999), Krysiński et al. (2000) and Czuba et al. (2002). Interpretations in the above-mentioned papers were based on 2-D modelling using forward modelling with a raytracing algorithm and tomographic inversion (Červený and Pšenčík, 1983; Hole, 1992).

The results of modelling along profiles P3 and P5 and the northeastern part of profile P4 supply information about crustal structure of the East European Craton. All velocity models of the crust for this area are characterized by nearly uniform horizontally layered structure. The crystalline crust consists of three parts: upper, middle and lower, with P-wave velocities of 6.1–6.4, 6.5–6.7 and 7.0–7.2 km/s, respectively. The crystalline basement lies at a depth of 0.5–5 km with the depth increasing greatly to the southwest as the edge of the craton is approached. The depth of the Moho ranges from 39–45 km in northeastern Poland up to 50 km beneath Lithuania. The sub-Moho P-wave velocity (P_n) is 8.05–8.1 km/s.

The crustal structure of the Polish basin and the Palaeozoic platform is represented by profile P1 and by the southwestern parts of profiles P2 and P4. Profile P1 is situated in the Polish basin area and it is oriented parallel to the EEC edge in a zone that has experienced Variscan deformation (Jensen et al., 1999). Profiles P2 and P4 cross the edge of the East European Craton almost perpendicularly. In general, the P-wave velocities of the upper crust in the Polish basin are low (<6.1 km/s) down to depths of almost 20 km. This thick pile of low velocity material can be interpreted as being sedimentary rocks with some volcanics and intrusions (Guterch et al., 1999). Below 20 km, the P-wave velocity is generally >6.8 km/s with some areas having high velocity gradients and strong ringing reflectivity. The velocity of the uppermost mantle is high (>8.2–8.3 km/s).

3. Seismic data and modelling method

The POLONAISE'97 experiment involved two instrument deployments but some instruments were located along each major profile (P1–P4) during each deployment. The survey was designed to obtain not only in-line recordings along the profiles, but also fan recordings of the off-line shots. The use of 613 seismic recorders and 64 seismic sources provided considerable but far from ideal 3-D ray coverage. The data from fan recordings covered the region between the lines of seismic profiles and allowed for construction of a 3-D model of the crustal structure. Examples of seismic record sections used as the source of the input data for tomographic inversion are presented in Figs. 2–5. The seismic sections show good quality recordings with clear first arrivals of P_g and P_n wave, usually up to a distance of 300–400 km. The Pg wave, with apparent velocities from 6.1 to 6.7 km/s, is observed at offsets from 0 to about 120 km in the area of the Palaeozoic platform, and from 0 to 200 km on the EEC. At larger offsets, P_n wave can usually be observed. The apparent velocity of P_n varies from 8.0 to 8.4 km/s, with highest values on the Palaeozoic platform (profile P1, Fig. 2). In some sections, arrivals with apparent velocity of 7 km/s are visible in the offset interval 120–150 km (Fig. 3). They may represent lower crustal refracted waves.

The iterative back projection package for tomographic inversion by Hole (1992) uses an efficient method of determining the seismic velocity distribution in a 3-D medium using first arrivals. The algorithm uses linearization of relation between the traveltime and the slowness. The velocity model is defined in a 3-D rectangular grid with equidistant nodes. The solution is sought iteratively. To obtain velocity perturbations, traveltime residuals for rays calculated in each iteration are uniformly distributed in cells crossed by seismic rays, then summed and smoothed.

For tomographic modelling, 10,950 picks of first arrivals were used (Fig. 6). The P-wave velocity model was defined at equidistant nodes of the 3-D rectangular grid. The distance between nodes (the cell size) was 2 km. The size of the model was $928 \times 368 \times 68$ km (depth) or $464 \times 184 \times 34$ cells. Thus, total number of cells in the model was almost 3 million.

The initial model used was a 1-D P-wave velocity distribution. An average traveltime curve was con-
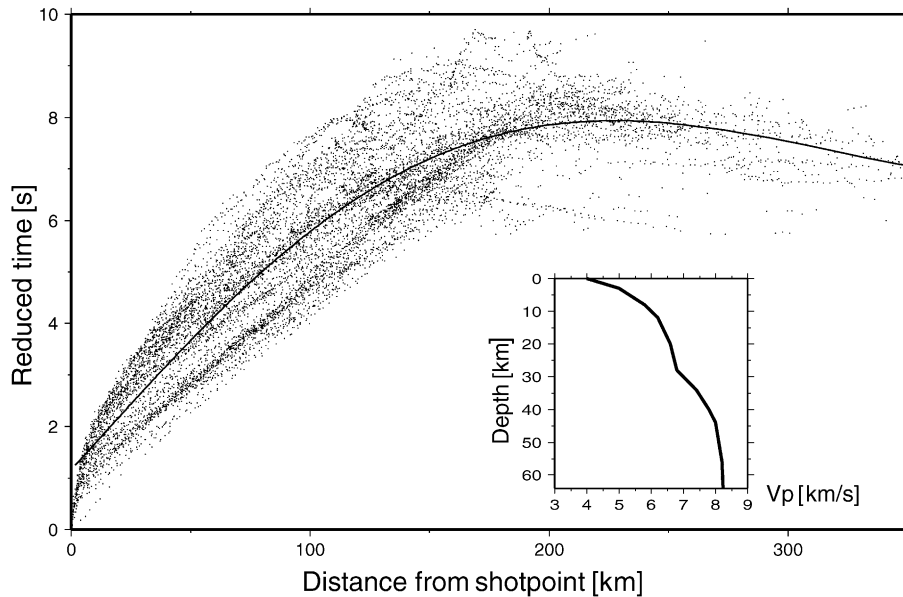
Fig. 6. Traveltime data of the first arrivals which have been used in 3-D inversion. Thin line is an average traveltime curve used for computation of a 1-D initial velocity model (right).

structed using all first arrivals traveltimes. Then, a 1-D velocity distribution for the average curve was calculated by 1-D trial-and-error modelling with the program LAUFZEIT (Kaminski and Müller, 1979), seeking a smooth velocity distribution with no first order discontinuities. In the first step of the computation, picks up to a distance of 40 km were used. In the next steps, this distance was increased in order to gradually enlarge the maximum depth of the ray penetration. This allowed for constraining shallow layers first, before modelling the deeper ones. In each step, several iterations were performed, with a decreasing size of the smoothing operator area. In this way, the resolution of the algorithm was gradually increased. In each inner loop with constant maximum offset and smoothing operator size, several iterations were performed in three nested loops using the following scheme:

- Outer loop over increasing maximum offset of picks used for modelling: 40, 80, 160, 300, 800 km.
- Middle loop over decreasing moving average smoothing operator sizes: 32 × 32 × 12, 16 × 16 × 6 and 8 × 8 × 4 cells.

- Inner loop: up to four iterations with constant maximum offset and smoothing operator size.

The iterations in the innermost loop were stopped when the RMS curve (root mean square average of differences between experimental and calculated travel times) started to flatten. The RMS value for the final model is 0.13 s.

4. Checkerboard tests

In order to evaluate the spatial resolution in the entire model area, checkerboard tests were performed. This type of test is commonly used in traveltime inversion problems to investigate the capability of the ray coverage obtained for a given data set to resolve velocity heterogeneities of a specified wavelength. An example of the application of the checkerboard test can be found in Zelt and Barton (1998).

The test procedure consisted of the following steps. First, an average model obtained for the given data set was perturbed with an alternating pattern of positive and negative P-wave velocity anomalies (± 0.15 km/ s) of rectangular shape (a checkerboard) that extended
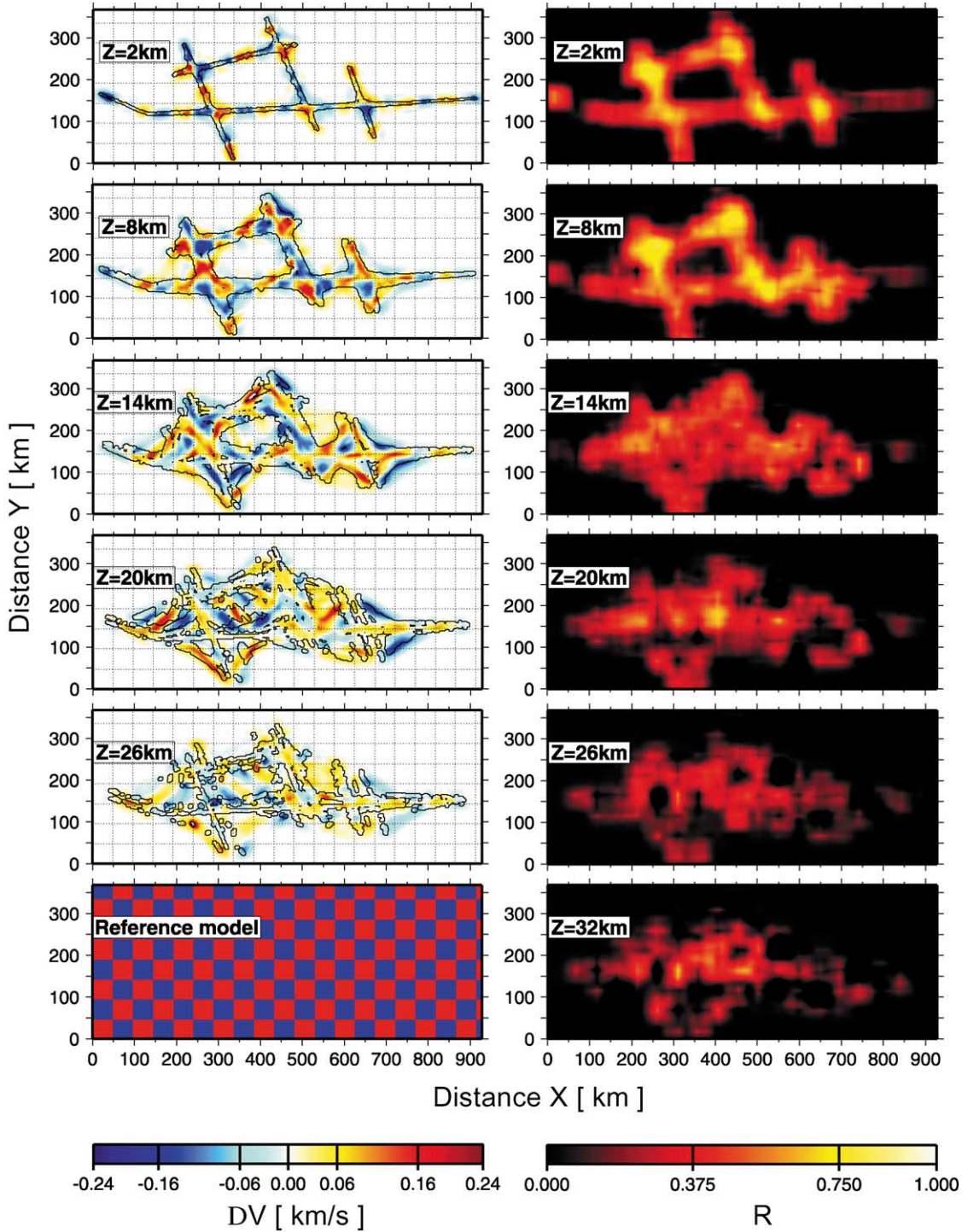
Fig. 7. Results of the checkerboard test for the anomaly size 48 km. Horizontal slices of the DV distribution (left) and resolvability (right).

vertically throughout the model with constant amplitude. The synthetic traveltimes were calculated for the perturbed model using the same source and receiver geometry as in the real experiment and random noise was added to traveltimes in order to simulate data errors. This random noise was Gaussian with a standard deviation of 0.1 s, slightly above the estimated level of the real traveltimes uncertainty.

The resulting synthetic data set was inverted in the same way as the observed traveltime data using the average (nonperturbed) model as the initial model. The result of the inversion (the recovered model) was then compared with the original model with the checkerboard velocity field. The similarity of the models was used as a measure of confidence for inversion results in different parts of the model. This procedure was applied for anomalies of different size (24, 48 and 96 km) in order to estimate the resolving

capability as a function of the size of the velocity inhomogeneities. The tests were performed with an iteration scheme similar to that for the real data, using eight iterations.

For presentation of the results, DV (the difference between the recovered and the original model) has been calculated and plotted in horizontal slices at various depths. The quality of the recovered model was estimated by visually comparing the recovered DV with DV for the original model. For quantitative assessment of the quality, plots of the resolvability, R, calculated as defined by Zelt and Barton (1998), who adapted a semblance operator for this purpose, have been used.

The results of the inversion for the 48-km anomaly grid for different depths are presented in Fig. 7 as horizontal slices through the model. Generally, the recovered model is, as expected, best resolved in the
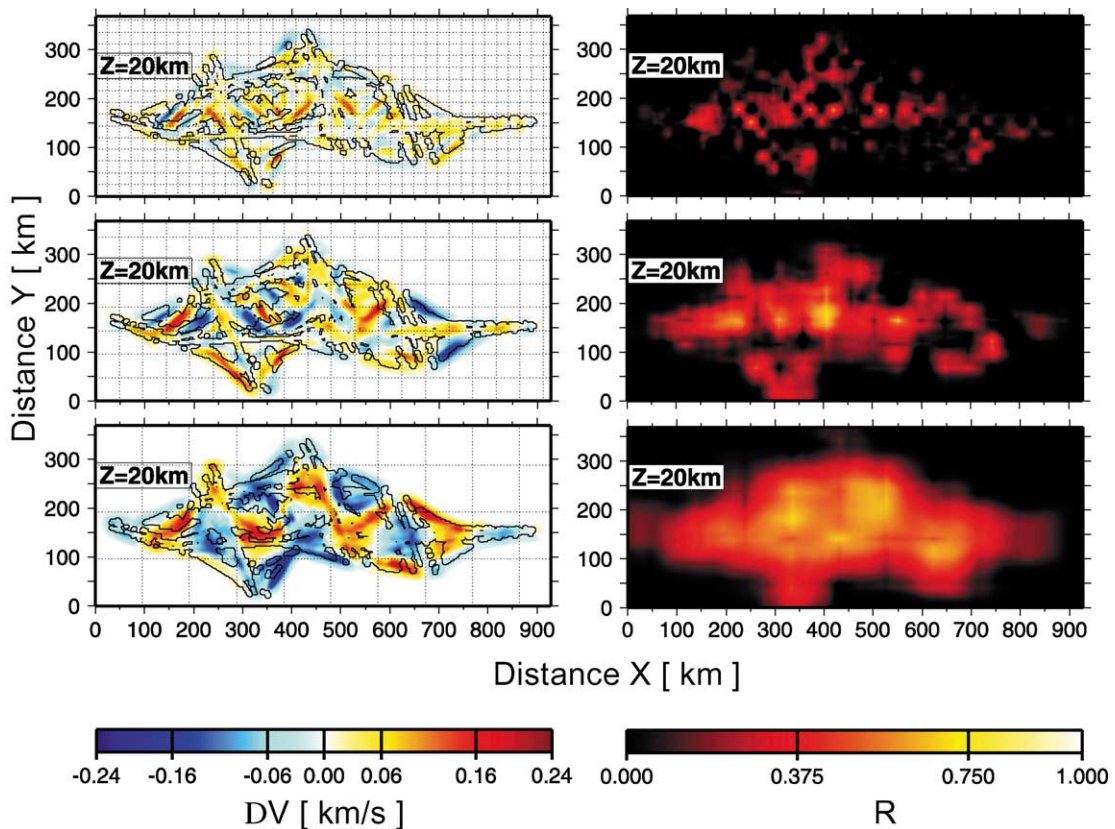
Fig. 8. Results of the checkerboard test for the anomaly sizes 24, 48 and 96 km at the depth of 20 km. Horizontal slices of the DV distribution (left) and resolvability (right).

areas of denser ray coverage. The model quality strongly correlates with depth and is the best in the 2–14-km range. At these depths, the recovered model shows good resemblance to the original, especially in the center of the ray-covered area. Near the borders of the nonzero ray density region, some artefacts created by low and anisotropic ray coverage are observed. At larger depths, the anomaly pattern is heavily distorted and only slightly resembles the original pattern.

The checkerboard tests allowed us to study the dependence of the resolvability on the scale of crustal inhomogeneities. A summary of the checkerboard test results showing the quality of the model as a function of the velocity anomaly size is shown in Fig. 8. The figure shows horizontal slices at 20-km depth. The anomalies with a size of 96 km are well resolved throughout the whole ray covered model area. The 48-km anomalies are mostly well recovered, except at the limits of the ray-covered area. For the smallest anomalies, 24 km, only a small part of the model in the region of maximum ray coverage is well resolved. For all anomaly sizes, the best resolved depth range is 2–14 km.

In summary, the checkerboard tests showed that for this experimental geometry we are able to resolve features with a size of the order of 100 km or larger in almost the whole area with ray coverage and features larger than 50 km at depths of 0–15 km. In a limited model area with very good ray density, inhomogeneities of about 30-km size can be detected.

From these results, we can estimate the optimal location of shots and receivers for future experiments. For example, the ray coverage of the shallow parts of the Polish basin would be improved by additional shotpoint (or short line of receivers) in the middle of the area between profiles P1, P2, P3 and P4. Additional shotpoint/receiver in the gap between profiles P3, P4 and P5 would also be helpful.

5. Modelling results

The final velocity distribution is shown in Figs. 9 and 10. The velocity model has been cut in 2-D slices in order to allow visual inspection of the 3-D volume. Velocity values for each node were plotted only if the ray density in the corresponding cell had a nonzero

value, in order to show the constrained areas only. For vertical slices, the ray density in an eight-cell wide area (32 km swath) around the cutting plane was summed to create a mask defining constrained areas in the given slice. This approach made it easier to compare the 3-D and 2-D results. The ray density at 20-km depth is shown in Fig. 9.

The velocity model obtained shows substantial horizontal variations of crustal structure across the study area, proving that the information about the crustal structure carried by the traveltimes data has been (at least partially) recovered in the inversion process. The results of the modelling reflect the complex structure of the Earth's crust in the TESZ region and provide insights about the physical characteristics of the tectonic units in the area.

The horizontal slices of the 3-D velocity distribution presented in Fig. 9 clearly show the differences between the areas of the Palaeozoic platform to the southwest, the Polish basin, and the East European Craton to the northeast. At a depth of 10 km, velocities of less than 6 km/s typical for sedimentary rocks are observed in the Polish basin and in parts of the Palaeozoic platform, while in the EEC area P-wave velocities at the same depth are higher than 6 km/s, the value characteristic of crystalline rocks of the upper crust. At 18-km depth, velocities lower than 6 km/s exist only in a very limited area, approximately marking the bottom of the basin. In the slice cutting the model at 30-km depth, the velocity distribution is distinctly different between the Palaeozoic platform which is characterised by velocities of 7 km/s or greater and the EEC with velocities of about 6.5 km/s. A similar differentiation between these areas can still be seen at a depth of 40 km where the velocities in the EEC area are consistent with the presence of lower crustal rocks, but velocities are significantly higher than 8.0 km/s in the platform area indicating the upper mantle has been penetrated.

This variability can also be seen on the vertical slices in the *Y*-plane (Fig. 10), especially for *Y* = 130 km, cutting the model near the location of the P4 profile. From SW to NE, the slice crosses the area of the Palaeozoic platform with relatively thin crust (about 35 km), the Teisseyre–Tornquist Zone (Polish basin) with a deep asymmetrical sedimentary basin and a relatively thin crystalline part of the crust, and
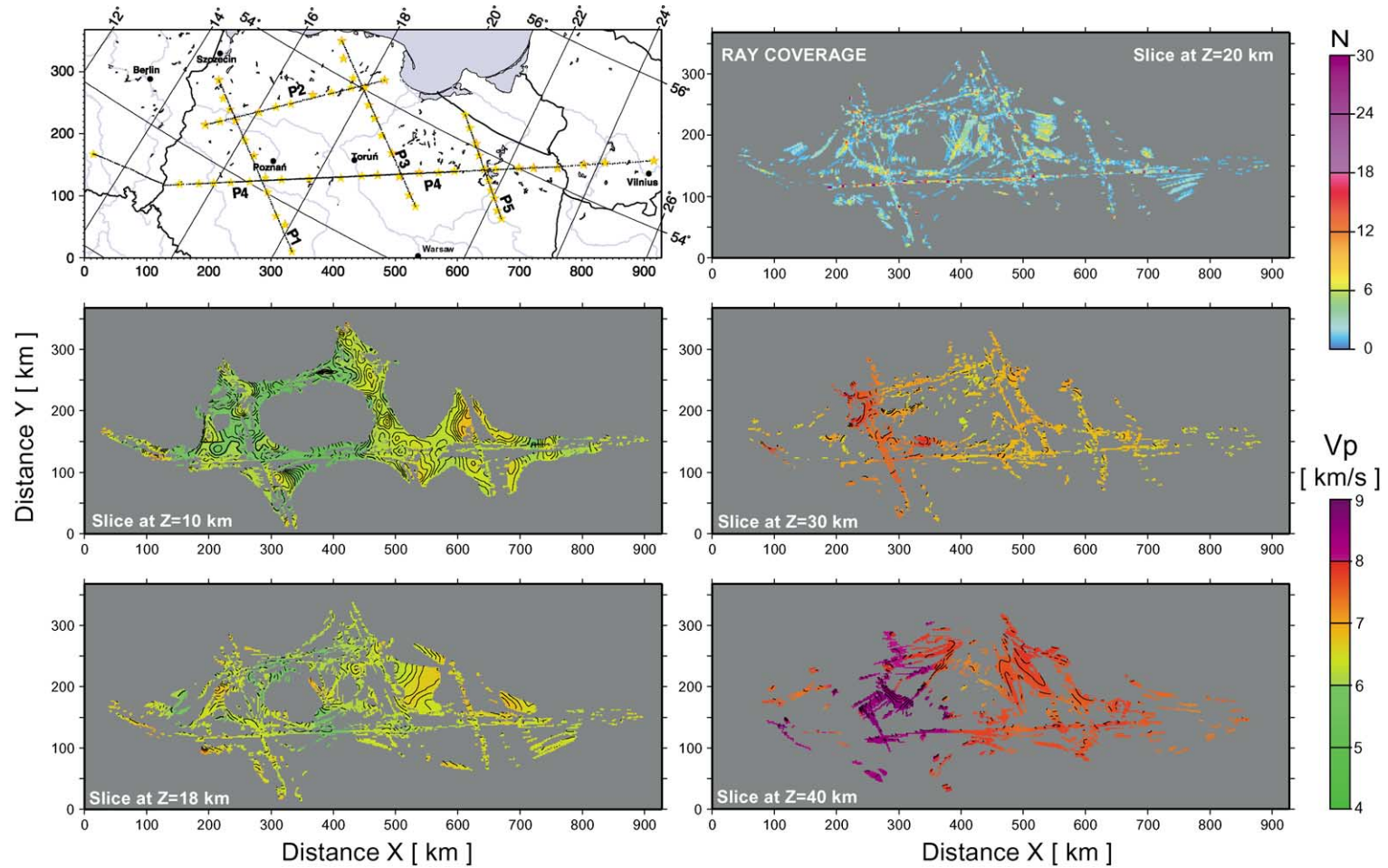
Fig. 9. Results of 3-D P-wave tomographic inversion for POLONAISE'97 data. Upper left rectangle shows a portion of the model with profile locations. Distance *X* and *Y* in kilometers (for bottom and left edge) and geographical coordinates (for the right and upper edge). Upper right rectangle shows ray density at 20-km depth. Below, next four rectangles show horizontal slices of the velocity distribution at depths *Z* = 10, 18, 30 and 40 km, respectively.
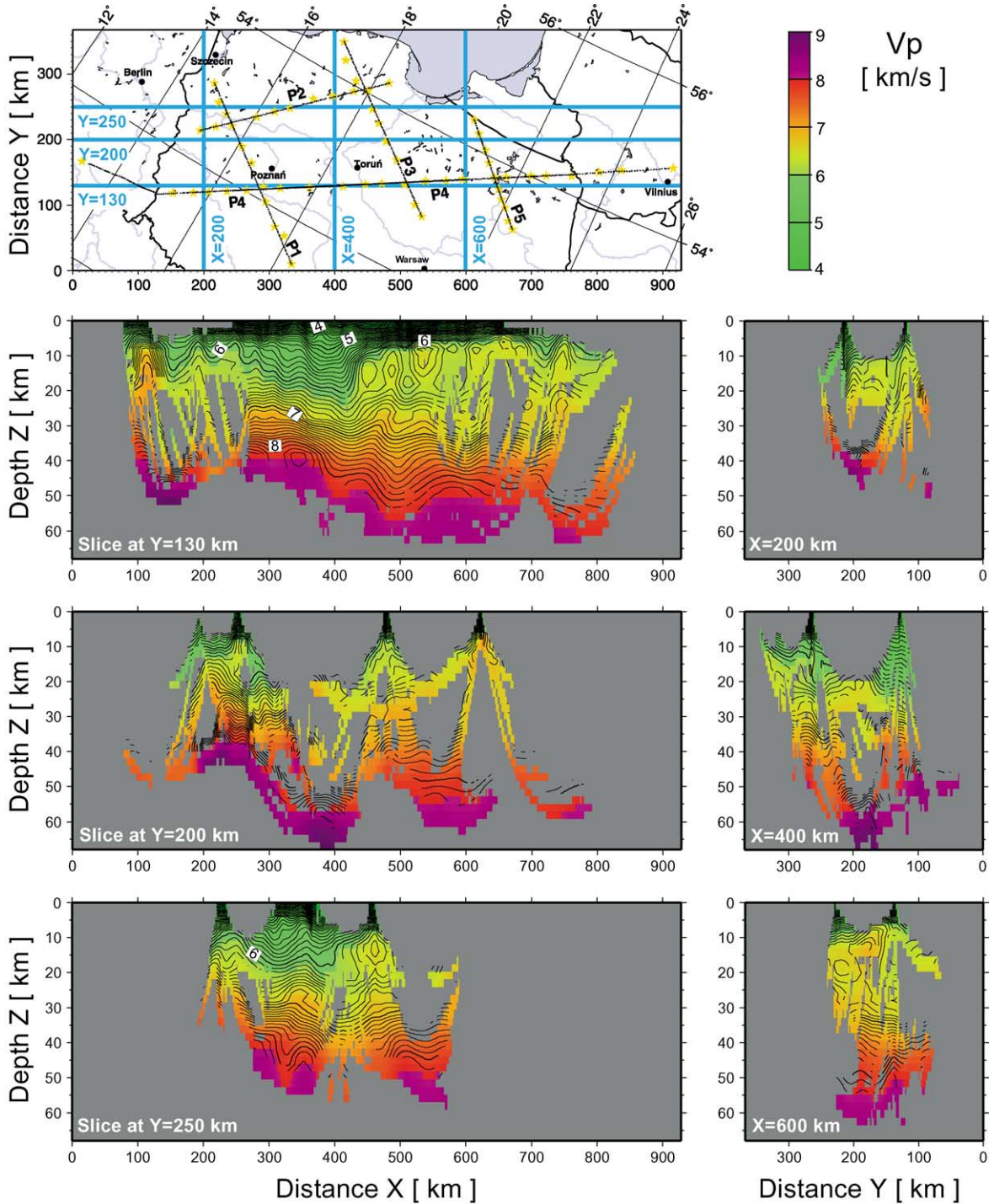
Fig. 10. Vertical slices of the 3-D velocity model along lines $Y = 130$, 200, 250 km and $X = 200$, 400, 600 km shown as blue lines on the map.

finally, the East European Craton with thin sedimentary cover and about 45-km thick crust.

Vertical slices in the *X*-plane are shown in Fig. 11, and a comparison of the 2-D model along profile P4 and the corresponding slice through the 3-D model is shown in Fig. 12. These slices demonstrate the advantages of a 3-D survey with fan recordings and 3-D modelling over 2-D modelling of in-line shots. In the 3-D model, we observe good ray coverage in many places between the profiles that provides useful constraints on the lateral extent of many velocity anomalies not provided by the 2-D approach. However, the short wavelength velocity anomalies observed in the 3-D model are the result of a smaller smoothing operator being used than in the derivation of the 2-D model.

When determining the depth of velocity discontinuities in the crust based on a tomographic model, it should be mentioned that the smoothing introduced by the modelling algorithm and the nature of the algorithm itself cause any velocity discontinuities present

to be represented as broad gradient zones. Thus, for example, the area with velocities >8 km/s occurring under the Moho discontinuity will be significantly shifted down in the tomographic model appearing to be deeper than in reality. This is due to lower crustal velocities being ''averaged'' with upper mantle velocities by the smoothing operator. Thus, the exact determination of the depth of velocity discontinuities based on tomographic inversion results is difficult. The position of a discontinuity can be estimated from the location of a high vertical velocity gradient zone, or from the location of a velocity isoline which is the average of the expected velocity values above and below the discontinuity.

In order to check the agreement between the obtained model and the data, an analysis of the traveltime residuals was conducted. The diagrams of traveltime residual distribution (Fig. 12) give more detailed information about the quality of the travel time fit with the data than the overall RMS value. The final distribution is centered on zero and shows
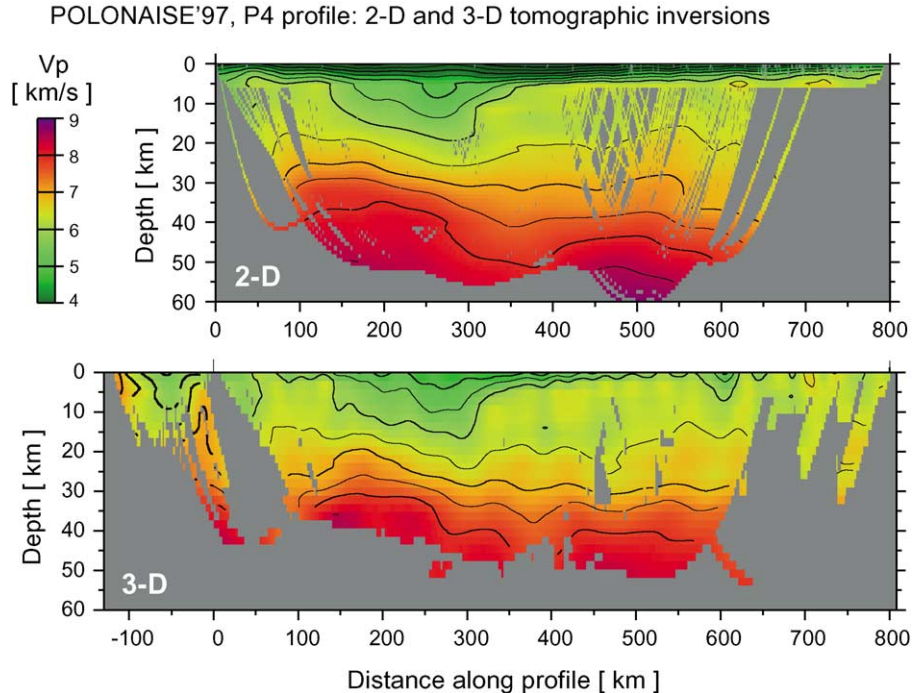
Fig. 11. Comparison of P-wave velocity tomographic models along profile P4 obtained by 2-D (upper) and 3-D (bottom) inversions. 'Zero' of 2-D profile at the Polish–German border corresponds to 123 km distance in the 3-D model.
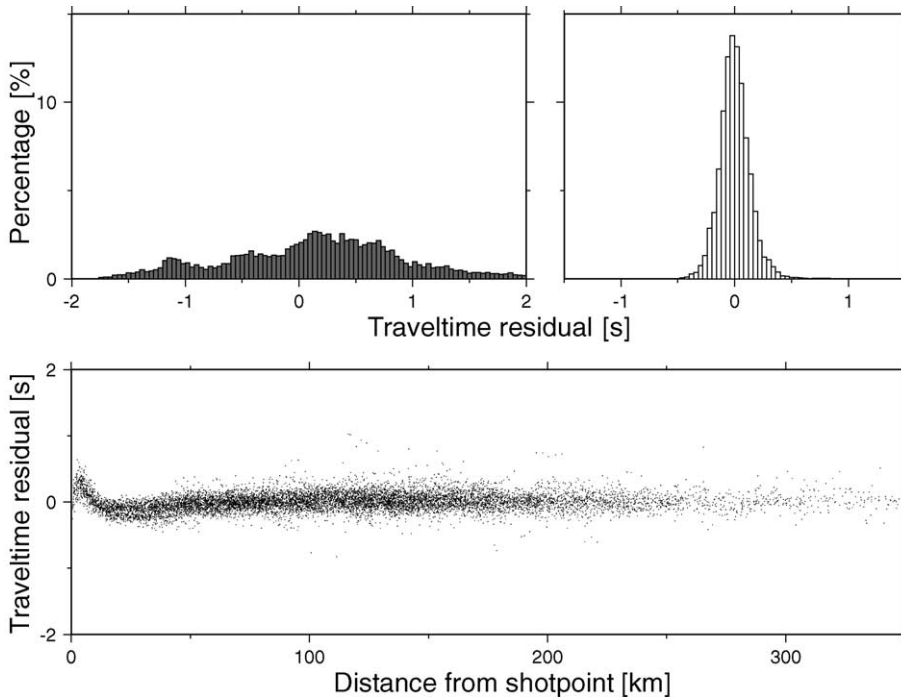
Fig. 12. Histogram of distribution of traveltime residuals for initial (upper left) and final (upper right) model and diagram of final traveltime residuals versus offset (bottom).

substantial improvement of the fit compared to the initial distribution of residuals. The plot of the residual values versus offset shows that they are rather uniformly distributed across the whole range of offsets and that the fitting errors are not due to some specific group of arrivals.

6. Summary and conclusions

Three-dimensional seismic modelling of crustal structure in the Trans European Suture Zone based on the data from the POLONAISE'97 experiment provides intriguing new details about the complex velocity structure in the transition zone between the Phanerozoic terranes of Central Europe and the East European Craton. The modelling results are most robust in the Polish basin region. The axis of the basin, the Mid-Polish Trough (MPT), is parallel and adjacent to the edge of the EEC. The base of the Permian in the MPT changes in depth from about 3000 m in the northwest to about 8000 m to the southeast (Karnkowski, 1999) and

the 3-D seismic modelling shows low (<6.1 km/s) velocities consistent with the presence of sedimentary rocks extend to a depth of about 20 km. The 3-D results indicate structural variations within the MPT. The shape of the Polish basin in the vicinity of the profile P4 shows significant asymmetry, with steep boundary in NE, defining the SW limit of the East European Craton, and gently dipping slope in SW. Near the profile P2, the bottom of the basin is almost horizontal. The NE boundary of the Polish basin is geographically well defined and linear along approximately 200 km length of the modelled area. In SW, the velocity model does not allow for precise delineating of the extent of the basin. The horizontal slice at 10-km depth shows irregular high velocity anomalies within the basin (Fig. 9). The anomaly at $X=300$ km, $Y=100$ km correlates with the southern part of the Wolsztyn ridge. In addition to the general observation that the crust in the region modelled is thickest beneath the EEC, the 3-D modelling suggests significant topography on the Moho (approximately located at 7.6 km/s velocity isoline) particularly in the Polish basin area. Three-

dimensional recording geometry allowed the tracing of the variations of the Moho depth not only along the profiles, but also between them (Fig. 10). The slice at $X = 400$ km shows about 10 km variation of the Moho depth over a 100-km interval, with crust thickening in direction to East European Craton. The slice at $Y = 200$ km, which also contains mainly rays from off-line records, clearly shows Moho topography similar to that along profile P4 ($Y = 130$ km), but with deeper crustal root beneath western part of the Polish basin. In the area of the East European Craton, in the northwestern part of profile P5, a body with high seismic velocities of about 6.6 km/s was found in the depth range 2–10 km, which coincides with the well known Kętrzyn anorthosite massif. Its relation to the surface geology and its location, determined from fan recordings along profiles P4 and P5, are discussed in detail by Czuba et al. (2002).

Our preliminary analysis also shows that three-dimensional images of the P-wave velocity distribution also provide insights about the source of magnetic and gravity anomalies in the Trans European Suture Zone region. For example, there are two large parallel gravity lows that extend along the boundary of the EEC (Krysiński et al., 2000). The one to the southwest is due to the low velocity (low density) sedimentary rocks in the MPT. However, the one to the northwest is in an area where the sedimentary cover is relatively thin. The 3-D modelling shows that velocities (and densities) are relatively low at mid-crustal levels suggesting that the source of this gravity anomaly is in the crystalline crust. Also, there is a complex gravity high in the area where profiles P4 and P5 intersect that correlates with high velocities in the upper crust.

The results of this 3-D seismic modelling of the POLONAISE'97 data will ultimately be supplemented by inversion of seismic data from previous experiments (profiles LT-4, LT-5, LT-7, TTZ), as well as other geophysical and geological data, to enhance our understanding of the tectonic evolution of the Trans European Suture Zone region in Central Europe.

References

Berthelsen, A., 1992a. Mobile Europe. In: Blundell, D.J., Freeman, R., Mueller, St. (Eds.), A Continent Revealed—The European Geotraverse. Cambridge Univ. Press, Cambridge, pp. 11–32.

Berthelsen, A., 1992b. From Precambrian to Variscan Europe. In: Blundell, D.J., Freeman, R., Mueller, St. (Eds.), A Continent Revealed—The European Geotraverse. Cambridge Univ. Press, Cambridge, pp. 153–164.

Berthelsen, A., 1998. The Tornquist Zone northwest of the Carpathians: an intraplate-pseudosuture. Geol. Foren. Stockh. Forh. 120, 223–230.

Červený, V., Pšenčík, I., 1983. Program SEIS83, Numerical Modelling of Seismic Wave Fields in 2-D Laterally Varying Layered Structures by the Ray Method (Software Package). Charles University, Prague.

Czuba, W., Grad, M., Luosto, U., Motuza, G., Nasedkin, V., POLONAISE P5 Working Group, 2002. Upper crustal seismic structure of the Mazury Complex and Mazowsze Massif, within the East European Craton in NE Poland. Tectonophysics 360, 115–128 (this volume).

Dadlez, R., 1989. Epicontinental Permian and Mesozoic basins in Poland. Kwart. Geol. 33, 175–198.

Grad, M., Janik, T., Yliniemi, J., Guterch, A., Luosto, U., Komminaho, K., Środa, P., Hoing, K., Makris, J., Lund, C.E., 1999. Crustal structure of the Mid Polish trough beneath TTZ seismic profile. Tectonophysics 315, 145–160.

Guterch, A., Grad, M., 1996. Seismic structure of the Earth's crust between Precambrian and Variscan Europe in Poland. Publ. Inst. Geophys. Pol. Acad. Sci. M-18 (273), 67–73.

Guterch, A., Grad, M., Materzok, R., Perchuć, E., 1986. Deep structure of the Earth's crust in the contact zone of the Palae-

ozoic and Precambrian Platforms in Poland (Tornquist–Teisseyre Zone). Tectonophysics 128, 251–279.

Guterch, A., Grad, M., Materzok, R., Perchuć, E., Janik, T., Gaczyński, E., Doan, T.T., Białek, T., Gadomski, D., Młynarski, S., Toporkiewicz, S., 1992. Laminated structure of the lower crust in the fore-Sudetic region in Poland, derived from seismic data. Phys. Earth Planet. Inter. 69, 217–223.

Guterch, A., Grad, M., Janik, T., Materzok, R., Luosto, U., Yliniemi, J., Lück, E., Schulze, A., Förste, K., 1994. Crustal structure of the transition zone between Precambrian and Variscan Europe from new seismic data along LT-7 profile (NW Poland and eastern Germany). C. R. Acad. Sci. Paris 319 (s. II), 1489–1496.

Guterch, A., Grad, M., Thybo, H., Keller, G.R., 1997. New international seismic experiment in the Polish Basin POLONAISE'97. Oil and Gas News, Special Issue for the 15th World Petroleum Congress, Beijing, China, vol. 7, pp. 86–93, Warsaw.

Guterch, A., Grad, M., Thybo, H., Keller, G.R., Miller, K., 1998. Seismic experiment spreads across Poland. EOS, Transactions, American Geophysical Union, 79 (26), 302, 305.

Guterch, A., Grad, M., Thybo, H., Keller, G.R., POLONAISE Working Group, 1999. POLONAISE'97—international seismic experiment between Precambrian and Variscan Europe in Poland. Tectonophysics 314, 101–121.

Hole, J.A., 1992. Nonlinear high resolution three-dimensional seismic travel time tomography. J. Geophys. Res. 97, 6553–6562.

Jensen, S.L., Janik, T., Thybo, H., POLONAISE Working Group, 1999. Seismic structure of the Palaeozoic Platform along POLONAISE'97 profile P1 in southwestern Poland. Tectonophysics 314, 123–143.

Kaminski, W., Müller, G., 1979. Program LAUFZEIT. University of Karlsruhe.

Karnkowski, P.H., 1999. Tektoniczny model Basenu Polskiego: implikacje dla poszukiwan naftowych. Conference: Geologia–Geofizyka–Geochemia: Techniki integracji dla poszukiwan naftowych, 18 May. B.G. GEONAFTA, Warsaw, pp. 25–31, Abstracts.

Krysiński, L., Grad, M., POLONAISE Working Group, 2000. POLONAISE'97 seismic and gravimetric modelling of the crustal structure in the Polish Basin. Phys. Chem. Earth 25 (4), 355–363.

Kutek, J., 1997. The Polish Permo-Mesozoic Rift Basin. IGCP Project No. 369 Comparative Evolution of Peri-Tethyan Rift Basins, Abstract Book. 4th Annual Meeting and Fieldtrip, 29 August–3 September 1997, Barcelona, Spain.

Pharaoh, T.C., England, R.W., Verniers, J., Żelaźniewicz, A., 1997. Introduction: geological and geophysical studies in the Trans-European Suture Zone. Geol. Mag. 134 (5), 585–590.

Środa, P., POLONAISE Working Group, 1999. P- and S-wave velocity model of the southwestern margin of the Precambrian East European Craton; POLONAISE'97, profile P3. Tectonophysics 314, 175–192.

Wernicke, B., 1981. Low-angle normal faults in the Basin and range province: nappe tectonics in an extending orogen. Nature 291, 645–647.

Wernicke, B., 1985. Uniform-sense normal simple shear of the continental lithosphere. Can. J. Earth Sci. 22 (1), 108–125.

Wessel, P., Smith, W.H.F., 1998. New, improved version of Generic mapping tools released. EOS, Trans., Am. Geophys. U. 79, 579.

Wilde-Piórko, M., Grad, M., POLONAISE Working Group, 1999. Regional and teleseismic events recorded across the TESZ during POLONAISE'97. Tectonophysics 314, 161–174.

Zelt, C.A., Barton, P.J., 1998. Three-dimensional seismic refraction tomography: a comparison of two methods applied to data from the Faeroe Basin. J. Geophys. Res. 103, 7187–7210.

Ziegler, P.A., 1990. Geological Atlas of Western and Central Europe. Shell International Petroleum, Maatschappij, 2nd ed. Geol. Soc. Lond. Elsevier, Amsterdam.